IUBAT Review—A Multidisciplinary Academic Journal, 7(2):64-84
https://doi.org/10.3329/iubatr.v7i2.78801

A Dumbbell-shaped Patch Antenna for IMD

Emtiaz Ahmed Mainul[1], Md. Faruque Hossain[2], Tawfikur Rahman[3,*], Nibedita Deb[4], Md.Moniruzzaman[3], S. M. Rezaul Karim[3], Md. Saidur Rahman[1]

[1]*Department of Electrical and Electronic Engineering, European University of Bangladesh, Dhaka, Bangladesh*
[2]*Department of Electronic and Communication Engineering, Khulna University of Engineering and Technology Bangladesh, Khulna, Bangladesh*
[3]*Department of Electrical and Electronic Engineering, International University of Business Agriculture and Technology, Bangladesh.*
[4]*College of Agricultural Sciences, International University of Business Agriculture and Technology, Uttara, Dhaka 1230, Bangladesh.*

Keywords:

Biomedical Applications;
Implantable Antenna;
Biotelemetry;
ISM;
MICS;
Inset-fed patch antenna.

Abstract

This paper presents a dumbbell-shaped patch antenna designed for biomedical applications. The antenna is powered through an insect-fed transmission line, and its resonance frequency is found within the Industrial, Scientific, and Medical (ISM) band, ranging from 2.3408 to 2.5546 GHz. The substrate of the antenna is chosen as FR-4 (with a relative permittivity of 4.3 and a loss tangent of 0.0004), while the superstrate, which isolates the radiating patch and ground, is made of Al_2O_3 (with a relative permittivity of 9.4 and a loss tangent of 0.004). The antenna design is simple, utilizing only a shorting pin to achieve the desired operating frequency of 2.444 GHz. To evaluate its performance as a transmitter antenna and its link budget with an external receiver antenna, the antenna is numerically constructed within a three-layer human tissue phantom consisting of skin, fat, and muscle layers. The proposed antenna, with compact dimensions of 8 × 5.5 mm², can communicate with the receiver antenna at a distance of approximately 9 m with 1 Mbps data speed. The antenna exhibits an impedance of 49.89–j0.16Ω, which is close to the desired source impedance of 50Ω. Furthermore, it demonstrates improved bandwidth, gain, and specific absorption rate (SAR) compared to some recent well-known papers.

1. Introduction

Wireless devices are very important to monitor human physiological parameters, e.g., blood pressure, temperature, glucose, etc. (Sukhija & Sarin, 2017). Many researchers have been concentrating on implantable medical devices (IMD) to monitor those physiological parameters, and send those data to the external device, and vice versa (Gayathri & Venkatanarayanan, 2021). Therefore, it is very essential to have an antenna in the IMD to send/receive data through wireless

[*]Corresponding author's E-mail address: tawfikur.eee@iubat.edu
Article received: 01 June, 2024 Revised and accepted: 18 Dec, 2024 Published: 31 Dec, 2024

links. The Medical Implant Communications Services (MICS) band (402–406 MHz) is mostly used to operate implantable antennas. The United States Federal Communications Commission (FCC) and the European Radiocommunications Committee (ERC) have validated this MICS band (Kiourti *et al.,* 2012). Besides, industrial, scientific, and medical (ISM) bands are also used for operating implantable antennas. The bands are in various ranges: 433–434 MHz, 868–868 MHz, 902–928 MHz, and 2.4–2.4835 MHz (Kiourti & Nikita, 2012). There is another band used for implantable antennas named Wireless Medical Telemetry Services, which ranges from 1.39–1.4 GHz (Valanarasi & Dhanasekaran, 2020).

Skin, serving as the interface between the antenna and the external environment, plays a crucial role in determining impedance matching and radiation characteristics. Its thickness and composition influence the penetration of electromagnetic waves into underlying tissues. Fat tissue, with its lower water content and conductivity compared to muscle tissue, contributes to reduced absorption and scattering of electromagnetic waves by the antenna. However, both fat and muscle tissues, each possessing distinct dielectric properties, affect antenna performance. Muscle, characterized by its high water content and conductivity, induces significant absorption and scattering, altering antenna impedance, radiation pattern, and efficiency. Understanding these tissue-specific influences is essential for optimizing the design and performance of implantable antennas in medical applications.Therefore,a researcher has to face lot of challenges to get optimum performance of implantable devices. As human body is a lossy medium due to high relative permittivity and high conductivity, it affects the performance of IMDs. The attenuation loss is increased with increasing permittivity and conductivity and attenuation constant is increased with those parameters. Also, in Van *et al.,* (2009) discussed the losses due to reflection from the boundary between adjacent two different tissues. Tissue conductivity increases exponentially with higher frequency, while permittivity decreases with higher frequency but is comparatively low. So, loss will be less at higher frequencies. The radiation pattern is broadened in lossy mediums in comparison with air (Moore, 1963). Also, radiation patterns change in symmetric and asymmetric anatomical body models. The polar radiation pattern exhibits significant variation between simulations conducted at the origin and those performed at distinct antenna positions. The implantable antennas are of compact size and exhibit narrow bandwidth. Frequency detuning happens in different body tissues, in different positions in the same body tissue, and in different orientations in the same body tissue. So, a large bandwidth is necessary.

Among all the challenges of implantable medical devices, antenna miniaturization is a prime concern. Using an antenna substrate of high permittivity will result in making the guided wavelength shorter, which will cause the resonance frequency to be lowered. The high permittivity substrate zirconia material ($\varepsilon_r = 27$, $\sigma \approx 0$, $\tan\delta \approx 0$) of thickness 0.05 mm is used in (Kaim *et al.,* 2020) for miniaturization purposes. The substrate of higher permittivity will affect radiation efficiency by converting antenna input power into surface waves

(Hussein & Mohammed, 2023). The refractive index says that it increases with increasing relative permeability (μ_r) and relative permittivity (ε_r) which causes effective propagation velocity to slow below the speed of light (Hendriks *et al.*, 2020). To minimize antenna size, a thin low-loss ferrite sheet layer ($\mu > 1$) has been used beneath a dielectric substrate (Lee *et al.*, 2015). This also affects radiation efficiency by converting antenna input power into surface waves. Besides, the utilization of a shorting pin facilitates to achievea quarter-wavelength microstrip patch antenna, similar to the resonance wavelength of a PIFA. Conversely, PIFA has low backward radiation, resulting in low gain, because currents at adjacent arms of the shorting pin and coaxial feeding line cancel each other. The most common miniaturization technique is lengthening the current path in the antenna radiator which helps the antenna to be resonated at a lower band. It can be done by designing various shapes within a certain area (Mainul & Hossain, 2021). The currents on the edges may cancel each other due to phase shift, which affects the antenna's performance. Antenna radiating-patch stacking on one after another superstrate can be used to lengthen the current path, but it increases overall thickness. Inductive or capacitive loading is used to match the impedance of the implantable antenna and also to minimize the imaginary part, i.e., the reactance of the antenna, which is required to get a compact antenna. The quality factor of an inductor or capacitor is the ratio of the reactance of an inductor or capacitor to its resistance at a given frequency. Every inductor or capacitor has its own resistance. So, a high Q factor is essential, but it decreases bandwidth (Stutzman & Thiele, 2012). Another way to match impedance is to make a defected ground structure (DGS), which helps alter the path of the return current. In (Mainul & Hossain, 2021), the impedance matches up to 48.87 + j 0.27 Ω by using DGS in the ground plane. Besides, DGS can be used as a miniature implantable antenna, because it slows the current by displacing the current path from one edge of the DGS to the other edge by changing phase shift. The easiest way to reduce the size of the antenna is to use a higher operating frequency. Therefore, the ISM band (2.4-2.483 GHz) is more commonly used to avoid the increased level of losses inside the human body.

It is must to make an IMD biocompatible, including implantable antennas, because human tissue is conductive and there is a chance for tissue damage through short circuiting between antenna metal and tissue. A thin insulating layer, either substrate or superstrate, is advantageous for low loss. The authors of (Gayathri & Venkatanarayanan, 2021) have used biocompatible polyamide (εr =4.3 and tanδ=0.004) for both the substrate and superstrate of the same thickness (0.05 mm) to reduce the overall dimension.Generally human tissue absorbs radiative power. If it happens in long time from implantable antenna, it may causes complex health issues. Human tissue absorbs antenna radiated power which is proportional to the electric field intensity (Singh & Kaur, 2021). So, it is necessary to find out the specific absorption rate (SAR)) to keep transmitted or received power within its allowable limit. The Federal Communication Commission (FCC) and Electronic Communication Committee (ECC) have

regulated that the specific absorption rate (SAR) must be equal to or lower than 1.6 W/Kg and 2 W/Kg, respectively, for 1g tissue standard and 10g tissue standard (Soliman *et al.*, 2021). It is very usual that the resonance frequency of implantable antennas can be varied from person to person for frequency shifting. It is required to have a wide bandwidth of implantable antennas to reduce the effects of frequency shifting. Various bandwidth enhancement techniques like parasitic patches, two-coupling radiating patches, etc. are being used. Two coupling radiating patch structures produce 68% bandwidth for the MICS frequency band (Soliman *et al.*, 2021).

Patients safety and interference issues are the prime reasons to limit the maximum allowable power, whose effects become lower, especially in the MICS band. But it is important to increase the gain for far field communication. But gain can be increased by modifying the radiation part using a meandered patch structure, an external lens, a parasitic ring, etc. The authors of (Xe *et al.*, 2020) found gain improvement up to 1.5 dBi by using walls around the radiating patch. If an implantable antenna resonates in the MICS and ISM bands, which is desired for antenna designers, the MICS band can be used for transferring data to an external device, while the ISM band can be used for giving 'wake up' signal to the IMD for saving its battery power (Duan *et al*., 2014). But if it resonates in the triple band, then the third band can be used for getting wireless power for the IMDs.

The overall dimension of an implantable antenna is around (6 × 5 × 0.5) mm^3 is found but it provides a high SAR value of 797.5 W/kg and a comparatively low bandwidth of 190 MHz at the 2.4 GHz frequency band. The authors of (Xe *et al.*, 2020) presented an implantable antenna operating at 2.45 GHz band, which provides a good bandwidth of 12.8 %, but the overall dimension of the implantable antenna is around (9.6 × 17 × 1.27) mm^3. An ISM band (2.4–2.5 GHz) antenna provides 3.2 dBi gain, but its dimension is larger (483.75 mm^3) which is presented. An implantable antenna resonates in the 915 and 2450 MHz bands, and its dimension is 24 mm^3 (Loktongbam & Koley 2020). But it provides comparatively low bandwidth (9.84 and 8.57%) and a higher SAR value of 971.56 and 807.34 W/kg in 1 g of standard tissue, respectively, in the two bands. In (Shah & Yoo 2018) , an implantable antenna demonstrated a lower SAR value of 18.5 W/Kg in a 1g standard tissue model at the 2.45 GHz band using ferrite sheet as a superstrate, but its overall dimension is a bit high (119.25 mm^3). So, the above discussions show that there are a lot of scopes to improve implantable antenna performances, especially for size, gain, bandwidth, return loss, SAR, etc.

This paper proposes the numerical design of a dumbbell-shaped implantable antenna that can resonate in the 2.444 GHz frequency band. The design is very simple, with ainset-fed transmission-line and a shorting pin. The performances are demonstrated inside a three-layer (skin, fat, and muscle) tissue phantom. The proposed implantable antenna is miniaturized and performs well in terms of bandwidth, gain, radiation pattern, and SAR value compared to some recent published literature. This paper is divided into the following sections: The

geometry of the antenna is described in Section 2; results and discussions is described in Section 3; and finally concluded in Section 4.

2. Material and methods

2.1 Geometry

The geometry of the proposed dumbbell-shaped antenna is shown in Figure 1(a)-(b). The copper material is chosen for its availability as a radiating patch in the proposed antenna. Its dimension is (width × length × thickness) 7.5 mm × 4 mm × 0.035 mm. FR-4 material (εr =4.3 and tanδ=0.0004) is chosen for its availability as antenna substrate. Its dimension is 8 mm × 5.5 mm × 0.29 mm. The copper is galvanized on both side of the substrate where the patch will be designed on one side and the other side will be the ground with same thickness of 0.035 mm. The ground is not manipulated but used for antenna port creation. To keep the implantable antenna isolated from human tissue, biocompatible alumina superstrate (ε_r =9.4 and tanδ=0.004) is used on top and bottom of the antenna.The thickness of the superstrate is chosen as 0.5 mm for its availability.

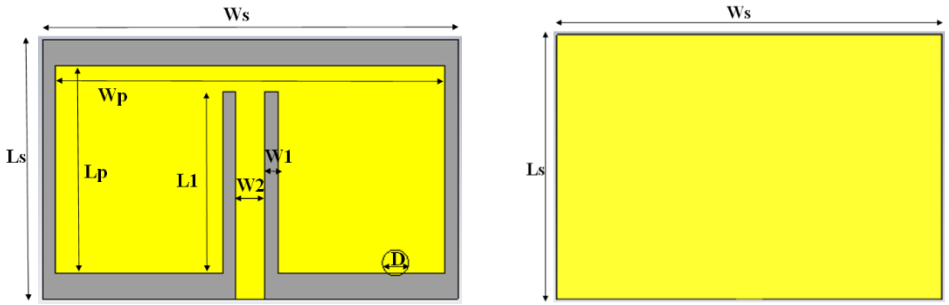

(a) (b)

Figure 1: Geometry of the proposed antenna: (a) radiating patch and (b) ground

The copper material is chosen for its availability as a radiating patch in the proposed antenna. Its dimensions are (width × length × thickness) 7.5 mm × 4 mm × 0.035 mm. FR-4 material (ε_r =4.3 and tanδ=0.0004) is chosen for its availability as an antenna substrate. Its dimension is 8 mm × 5.5 mm × 0.29 mm. The copper is galvanized on both sides of the substrate, where the patch will be designed on one side and the other side will be the ground with the same thickness of 0.035 mm. The ground is not manipulated but is used for antenna port creation. To keep the implantable antenna isolated from human tissue, biocompatible alumina superstrate (ε_r =9.4 and tanδ=0.004) is used on the top and bottom of the antenna. The thickness of the superstrate is chosen as 0.5 mm for its availability. The antenna impedance matching is completed by resizing the transmission line, So, the optimized size is (0.75 mm × 0.5 mm) with corresponding source impedance of 50 Ω. The details of the antenna parameters are shown in Table 1.

Table 1: Antenna Parameters

Parameter	Value (mm)
Ws	8
Ls	5.5
Wp	7.5
Lp	4
D	0.25
L1	1.9
W1	0.25
W2	0.5

In this scenario, a designed antenna is being rigorously evaluated within a numerical three-layered phantom model that simulates human body tissues. This model comprises three distinct layers, typically representing skin, fat, and muscle. The antenna is strategically placed within the fat layer, positioned between the skin and muscle layers, allowing for a comprehensive assessment of its radiation performance. Notably, the choice of phantom size is pivotal in this experiment, with a relatively large dimension of 100 mm × 100 mm × 24 mm selected as shown in Figure 2.

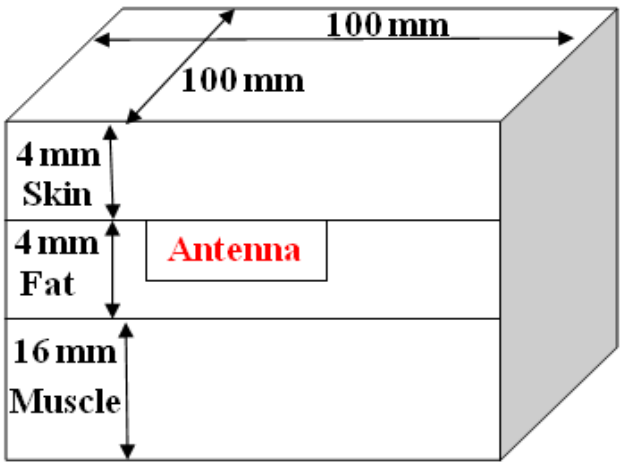

Figure 2: Cubic phantom model for the proposed antenna.

This larger size is significant as it ensures that the antenna's behavior is evaluated in conditions that closely resemble real-world scenarios. Such meticulous testing is essential for verifying the antenna's functionality and safety in its intended application, whether it be in wireless communication, medical devices, or other electromagnetic technologies. This passage describes a controlled experimental setup where a designed antenna is being tested within a simulated model of human body tissues to assess its performance in a specific context, taking into consideration the size and positioning of the antenna within the model. Such testing is important to ensure that the antenna functions effectively and safely in its intended application, which may involve communication, medical

devices, or other wireless technologies. In this context, the CST 2018 simulator is employed as a powerful tool to simulate the behavior of the proposed antenna. Simulating antennas is crucial, particularly when dealing with implantable antennas, as they interact significantly with human tissue. The electromagnetic properties of human tissues, such as skin, fat, and muscle, play a critical role in determining how the antenna will perform within the body.To accurately model these interactions, the simulator utilizes data on the dielectric permittivity and conductivity of these tissues, which are obtained from a reference source, as shown in Table 2. This property, represented by a numerical value, indicates how well a material can store electrical energy in an electric field. In the context of human tissues, it varies considerably. For instance, skin has a dielectric permittivity of 38.007, fat has a value of 5.28, and muscle has a higher value of 53.574 at 2.45 GHz. These values reflect the tissues' ability to interact with electromagnetic waves at this frequency.

Table 2: Tissue Properties at 2.45 GHz

Tissue	**Dielectric permittivity**	**Conductivity** (S/m)
Skin	38.007	1.464
Fat	5.28	0.105
Muscle	53.574	1.810

Conductivity (S/m) property measures how well a material conducts electricity. It's also a crucial parameter for antenna simulations. In this case, skin has a conductivity of 1.464 S/m, fat has a lower conductivity of 0.105 S/m, and muscle exhibits a higher conductivity of 1.810 S/m at 2.45 GHz. These values reflect the ability of these tissues to transmit electric current when exposed to electromagnetic fields.By incorporating these specific dielectric permittivity and conductivity values into the simulation, the CST 2018 simulator can accurately predict how the proposed antenna will function when placed within the human body. This level of detail and precision is essential when designing implantable antennas to ensure they perform effectively and safely within the complex electromagnetic environment of the human body at the specified frequency of 2.45 GHz.

3. Results and Discussions

3.1 Parametric result analysis

The results of the simulations reveal crucial performance metrics such as bandwidth and return loss. The antenna's bandwidth, measured at 213 MHz, indicates the range of frequencies over which the antenna can effectively operate within the ISM band. A wider bandwidth often implies better performance and versatility for various applications. In addition, The return loss of -54.72 dB at the 2.444 GHz frequency band, as depicted in Figure 3, is a crucial parameter.

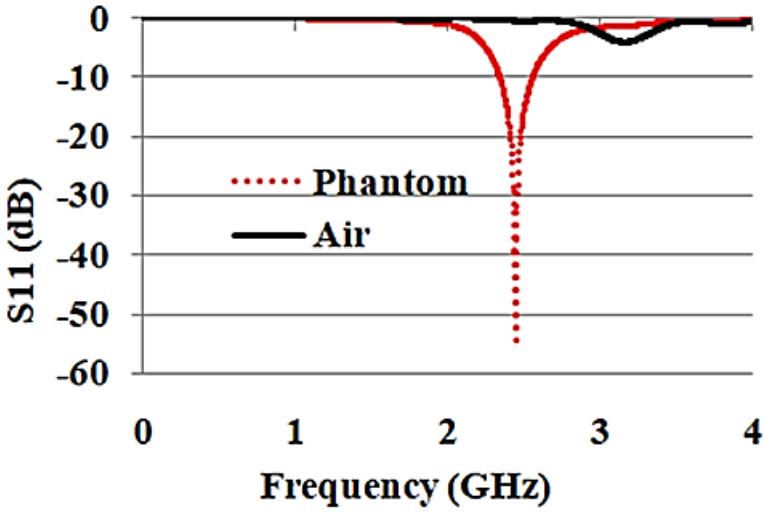

Figure 3: Simulated return loss (S_{11}) comparison between free space and inside phantom.

It quantifies how efficiently the antenna transmits power to the environment at its operating frequency. A lower return loss indicates that less power is reflected back into the antenna, signifying better energy transfer and performance.The passage highlights the importance of achieving a low S_{11} dB value, well below -10 dB, during simulation to attain the desired bandwidth coverage in practical applications. This requirement is based on the observation that simulated results often differ from measured results, and the latter typically exhibit a decrease in performance. By aiming for a significantly low S_{11} dB in simulations, engineers and designers can account for potential discrepancies between simulated and real-world performance, ensuring that the antenna will meet its operational requirements when used in actual human tissue environments.

The proposed implantable antenna exhibits distinct performance disparities between its operation inside a human-tissue phantom and in free space, emphasizing the profound influence of human tissue layers on its behavior. Within the phantom, the antenna excels due to its tailored design, which considers the electromagnetic properties of tissues, enabling effective signal transmission and reception for medical and wireless applications. Conversely, in free space, the antenna underperforms, potentially due to its non-optimization for such scenarios. This discrepancy highlights the importance of custom antenna designs that accommodate specific environments. Antennas for implantation must factor in tissue dielectric properties and conductivity. The consistency of these findings with prior studies reinforces the need to acknowledge how varying environments impact antenna performance. In summary, specialized antenna designs are imperative, adapting to the electromagnetic properties of the deployment environment, whether it's human tissue for implants or free space for other applications, ensuring optimal performance in practical settings.The performance

of the proposed antenna hinges on a critical component known as the shorting pin, which serves multiple essential functions in the antenna design. The shorting pin plays a pivotal role in increasing the current flow between the radiating patch and the ground plane of the antenna. This enhanced current flow is fundamental for the antenna's efficient operation. When the current flows more effectively between these two elements, it results in improved radiation characteristics and overall antenna performance. Another crucial function of the shorting pin is impedance matching. It helps match the impedance of the antenna with that of a 50Ω source. Achieving this match is vital for efficient power transfer between the antenna and the source, minimizing signal reflection, and maximizing signal transmission. Impedance matching ensures that the antenna is properly loaded, optimizing its performance in terms of both radiation efficiency and bandwidth.Resonance at 2.444 GHz: Figure 4 in the context of the antenna design highlights that the shorting pin is the key feature responsible for resonating the antenna at the desired frequency of 2.444 GHz. Resonance is a critical aspect of antenna operation as it ensures that the antenna efficiently radiates and receives signals at the specified frequency. Without the shorting pin, the antenna fails to exhibit any resonance frequency and instead shifts its operating frequency towards the left, indicating a lack of suitable performance at the intended frequency.

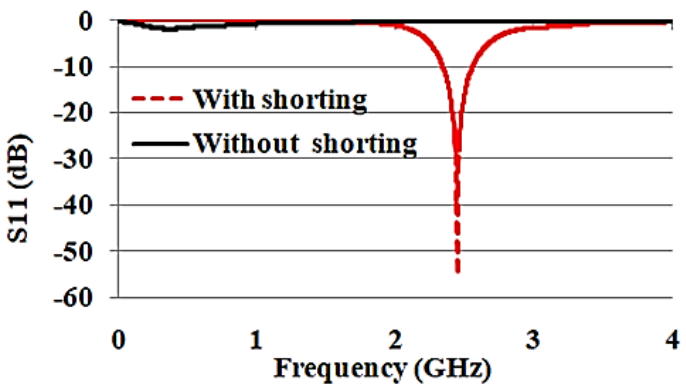

Figure 4: Effects of shorting pin on proposed design.

In essence, the shorting pin in the proposed antenna design is a vital component that not only enhances current flow and facilitates impedance matching but also serves as the primary means to achieve resonance at the target frequency. Its absence leads to a shift in the antenna's operating characteristics, rendering it ineffective for its intended purpose. Therefore, the shorting pin is a key feature that ensures the antenna operates optimally, providing the desired radiation performance and impedance matching necessary for its successful integration into various applications.

The voltage standing wave ratio (VSWR) is a critical parameter when assessing how efficiently an antenna utilizes reflected power from the antenna to the source. Achieving a perfect impedance match is essential for optimal

performance, and the ideal VSWR ratio falls between 1 and 2. In the case of the proposed antenna, the results are particularly noteworthy. Figure 5 demonstrates that the antenna achieves an excellent VSWR of 1.004 at 2.444 GHz.

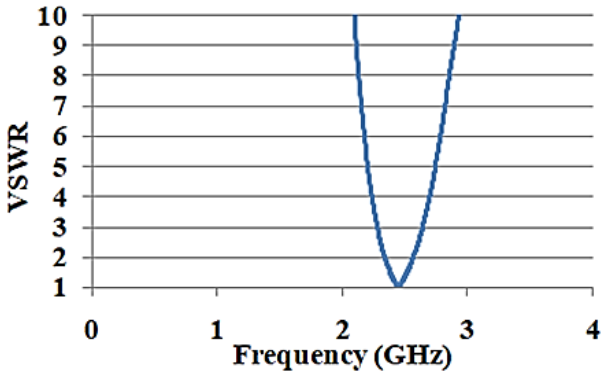

Figure 5: VSWR performance of the proposed antenna.

This exceptional VSWR value indicates an exceptionally close impedance match between the antenna and the 50 Ω source. In practical terms, this means that very little power is reflected back to the source when the antenna is operating. The majority of the power is efficiently transmitted from the source to the antenna, which is a highly desirable outcome in antenna design. Moreover, the performance of the proposed antenna is influenced significantly by transmission-line impedance matching effects. Figure 6 reveals that the antenna's transmission-line impedance is determined to be 49.89 – j0.165 Ω. This precise impedance value signifies that the antenna's transmission line is effectively matched to the source impedance of 50 Ω, further confirming the excellent impedance matching characteristics of the antenna.

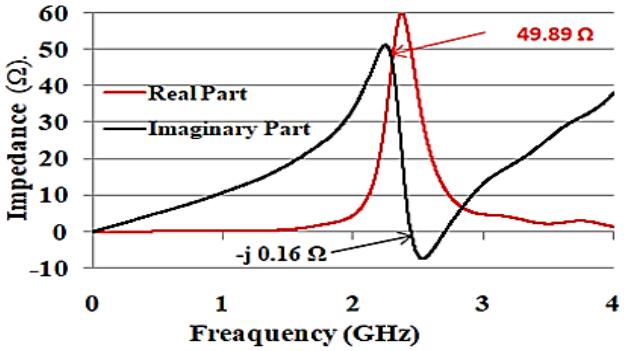

Figure 6: Impedance matching performance (real and imaginary part) of the proposed antenna.

In essence, the low VSWR and the close match between the antenna's transmission-line impedance and the source impedance indicate that the proposed antenna efficiently utilizes power, with minimal reflection, and is well-matched to the 50 Ω source, ensuring optimal performance in terms of signal transmission and reception. These results validate the antenna's suitability for its intended

applications, where impedance matching and efficient power utilization are of paramount importance.

The performance of the proposed antenna is influenced by two key design parameters: the width (W1) and length (L1) of the gap between the inset-fed transmission line and the patch. Although the antenna design is inherently straightforward, its performance is intricately tied to these specific dimensions. The proposed antenna design is characterized by its simplicity, but it employs an inset-fed configuration. In an inset-fed antenna, the feed point is located within the radiating element (in this case, the patch), and the dimensions of the gap between the feed and the patch significantly impact its operation. Figure 7 (a-(b) illustrates that changes in the width (W1) and length (L1) of this gap result in shifts in the antenna's resonance frequency. Specifically, as the width (W1) increases, the resonance frequency shifts to the left, indicating that the frequency at which the antenna operates effectively decreases. Conversely, changes in the length (L1) of the gap shift the resonance frequency to the right, implying an increase in the effective operating frequency.To achieve the desired resonance frequency for the antenna, the values of W1 and L1 need to be carefully optimized. According to the results presented, the optimized values for these parameters are determined to be W1 = 0.25 mm and L1 = 1.9 mm.

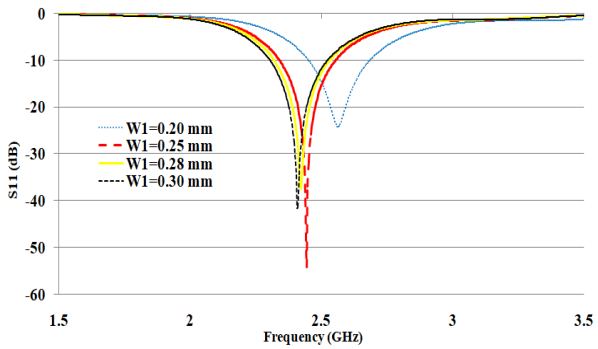

(a)

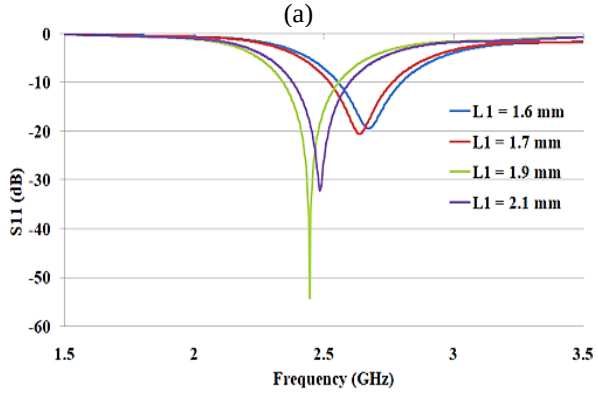

(b)

Figure 7: Parametric analysis of (a) W1 and (b) L1.

These values have been chosen to ensure that the antenna resonates precisely at the intended frequency, aligning with its design specifications. The dimensions of the gap between the inset-fed transmission line and the patch in the proposed antenna play a pivotal role in determining its resonance frequency. The antenna's design simplicity belies the intricate considerations required to achieve the desired operating frequency. The optimized values of W1 and L1, as determined through experimentation and analysis, ensure that the antenna operates at its intended frequency, making it well-suited for its specific application or communication requirements.

The results, presented in Figure 8 and Figure 9, provide valuable insights into the radiation characteristics and performance of the proposed antenna at its resonant frequency of 2.444 GHz. Figure 8 illustrates the simulated 3D radiation pattern of the antenna. The gain of -20.3 dB indicates how efficiently the antenna radiates electromagnetic energy in different directions. In this case, the radiation is primarily directed towards the +z plane, indicating that the antenna exhibits directional characteristics with a preference for radiating in a specific direction.

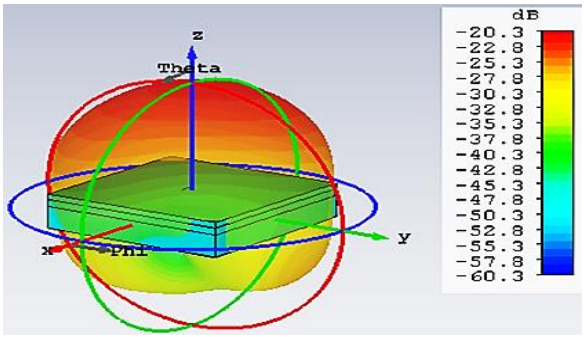

Figure 8: Simulated 3D radiation pattern of the proposed antenna.

The antenna's efficiency, measured at -27 dB, represents the proportion of input power that is effectively radiated as electromagnetic waves. Higher efficiency values imply more effective use of input power for radiation. Implantable antennas face challenges in achieving optimal gain and radiation pattern due to limited space, surrounding biological tissues affecting wave propagation, tissue absorption losses, impedance mismatch, and suboptimal antenna placement. These factors collectively lead to deviations from desired performance characteristics. Addressing these challenges requires a nuanced understanding of electromagnetic interactions with biological tissues and careful antenna design considerations.Moreover, the directivity of 6.73 dB quantifies the antenna's ability to concentrate its radiation in a particular direction. Higher directivity values suggest that the antenna focuses its radiation more effectively in its desired direction

Figure 9 (a)-(b) presents the radiation patterns of the antenna at its resonant frequency of 2.444 GHz. These patterns describe how the antenna

distributes electromagnetic energy in the horizontal (E-plane) and vertical (H-plane) planes. The E-plane radiation pattern exhibits a directive nature, indicating that the antenna predominantly radiates in specific directions within the horizontal plane. The presence of small side lobes at -11.7 dB suggests that there is some minor radiation in directions other than the main beam.Similarly, the H-plane radiation pattern shows directive characteristics with small side lobes at -7.2 dB. This means that the antenna concentrates its radiation within the vertical plane, with limited energy radiated away from the main beam.The choice of a directive radiation pattern for the proposed antenna is highlighted as advantageous for communication with a receiver antenna. Directive patterns focus the radiation towards the desired target, reducing interference and improving signal strength in the intended direction. This is particularly valuable in scenarios where minimizing interference effects during communication is essential, as compared to omni-directional antennas that radiate energy uniformly in all directions. The radiation pattern results indicate that the proposed antenna exhibits directional characteristics, with focused radiation in specific planes and relatively low side lobes. These characteristics make it well-suited for applications where interference reduction and signal concentration are critical, enhancing its effectiveness in wireless communication scenarios.

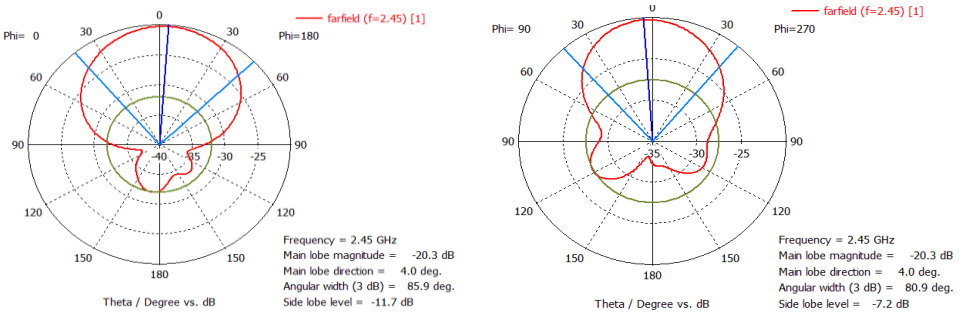

(a) (b)

Figure 9: Polar radiation pattern, (a) Phi = 0 deg and (b) Phi = 90 deg.

The results depicted in Figure 10 provide insight into the surface current distribution of the implantable antenna at its resonant frequency of 2.444 GHz. This distribution of current across the antenna structure is essential in understanding how the antenna radiates electromagnetic waves and how its design influences radiation patterns. The surface current distribution map reveals how electric charge moves along the antenna structure at the specified frequency. In this case, the antenna's currents are primarily concentrated on the right side of the antenna. This concentration of charge is a result of the shorting configuration applied to that side of the antenna.The shorting pin, which is located on the right side of the antenna, plays a crucial role in creating this charge concentration. It effectively bridges or connects the radiating patch on the right side to the ground plane. As a result, a closed loop is formed among the right-sided radiating patch, the shorting pin, and the ground plane. This closed loop configuration reduces the

radiation emitted from the right side of the antenna.In contrast, the left side of the antenna exhibits a different behavior. Charges on the left side of the antenna oscillate in time, which means that they are dynamically changing their positions. This dynamic charge movement on the left side leads to the generation of significant radiation from that side of the antenna.

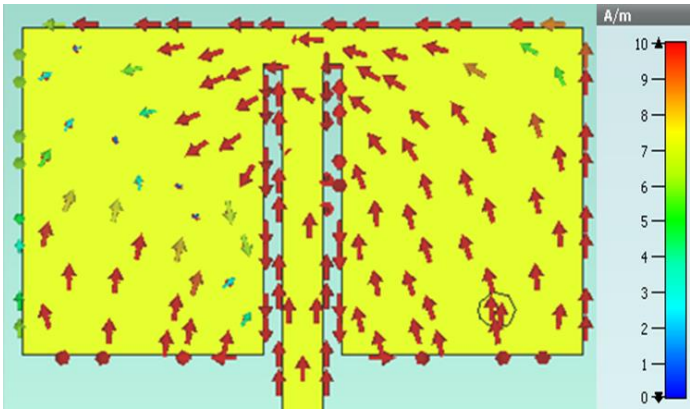

Figure 10: Surface current distribution at at 2.444 GHz.

The surface current distribution results show that the implantable antenna's design, particularly the presence of the shorting pin and the resulting closed loop on the right side, has a noticeable impact on charge distribution and radiation patterns. The concentration of charge on the right side minimizes radiation from that direction, while the dynamic charge movement on the left side results in substantial radiation from the left. Understanding these current distributions is crucial for optimizing the antenna's performance and radiation characteristics, ensuring that it meets the requirements of its intended applications, which may include wireless communication or medical devices.

3.2 Specific Absorption Rate distribution

The specific absorption rate (SAR) calculation is a critical aspect of antenna design, especially in the context of ensuring patient safety. SAR measures the rate at which electromagnetic energy is absorbed by the human body when exposed to electromagnetic fields, and it's an essential consideration for implantable antennas.To address patient safety concerns, the IEEE C95.3 standard is employed during simulation to analyze SAR. This standard provides guidelines for assessing the absorption of electromagnetic energy in biological tissues. During the simulation, the antenna is powered with 1W of input power as the source power, which represents the power level typically used in such assessments.SAR calculation involves two standards: the 1g average standard and the 10g average standard. These standards are used to measure SAR in different ways, considering different tissue masses. Figure 11(a)-(b) displays the SAR values for the proposed antenna, which are found to be 558 W/kg and 63.9 W/kg according to the respective standards.

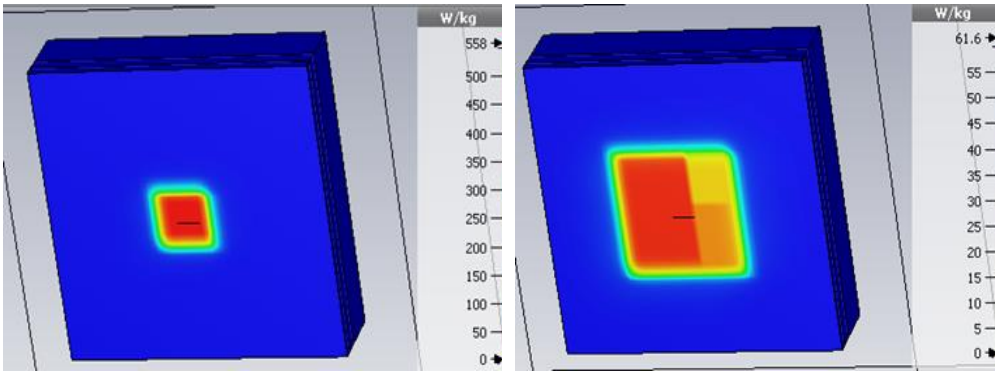

(a) (b)

Figure 11:. Simulated SAR calculation (a) 1g-standard (b) 10g-standard.

The SAR values obtained are crucial for determining the antenna's safety and performance. A low SAR value indicates that the antenna's electromagnetic energy absorption by the body is minimal, enabling the possibility of providing higher input power to the antenna. Conversely, if the SAR value is high, it suggests that the electromagnetic energy absorption is significant, necessitating lower input power to maintain safe levels. Table 3 provides valuable insights by indicating that the input power to the antenna should ideally be between 2.9 mW and 32.5 mW to adhere to SAR limits and ensure patient safety. Staying within this power range allows the antenna to function efficiently while maintaining safety standards.

Table 3: SAR Calculation and Accepted Input Power at 2.444 GHz

IEEE Standard (IEEE C95.3)	Max. Average SAR (W/Kg)	Max. Allowable Input Power (mW)
1g-avarage	558	2.87
10g-avarage	61.6	32.5

Transmitted Power and Output Power: It's worth noting that external considerations, such as standards set by the European Research Council (ERC), play a role in determining the acceptable power levels for implantable medical devices (IMD). In this context, the transmitted power is set at 46.02 dBW (25 µW), while the output power of the transmitter antenna should be 3.2 µW (-25 dBm) according to reference (Huang & Kishk, 2011). SAR calculations are crucial for evaluating the safety and performance of implantable antennas. By adhering to safety standards and optimizing input power levels within specified ranges, designers can ensure that these antennas operate effectively while prioritizing patient safety in applications such as medical implants or other wireless devices that interact with the human body.

3.3 Communication Link

The establishment of far-field communication between a transmitter (Tx) and a receiver (Rx) requires a thorough analysis of the link budget to ensure optimal signal quality and reliability. This link budget can be calculated using specific equations provided in reference (Hout & Chung, 2019). The design assumptions and parameters for the proposed implantable antenna's link budget are provided in Table 4. These include specific values for antenna gains, path loss, distance, and other parameters that are crucial for assessing the communication performance and ensuring that the link budget meets the desired criteria.

Table 4: Link Budget Parameters

Transmitter	**Values**	**Transmitter**	**Values**
Central Frequency (MHz)	2444	**Signal quality**	
Transmitted power, Pt (dBW)	−46.02	Bit rate, Br (Mbps)	10
Gain, Gt (dBi)	−20.3	Bit error rate	$1.00E^{-05}$
EIRP (dBW)	−66.32	Eb/No (ideal PSK) (dB)	9.6
Receiver		Coding gain, Gc (dB)	0
Gain, Gr (dBi)	2.15	Fixing deterioration, Gd (dB)	2.5
Temperature, T °(K)	293		
Boltzmann constant, K	$-1.38E^{-23}$		
Noise power density, No (dB/Hz)	−203.93		

It's important to note that this analysis assumes simplified conditions by ignoring factors like polarization mismatch losses and impedance mismatch losses. These simplifications allow for a straightforward assessment of the link budget. Additionally, the use of a linearly polarized dipole antenna with a specified gain simplifies the receiver antenna model. The link budget analysis is a vital step in evaluating the communication performance of the proposed implantable antenna. It considers various parameters to ensure that the communication link operates reliably and efficiently, taking into account the specific characteristics of the antenna and the communication environment.

The results presented in Figure 12 provide valuable insights into the link margin calculation for the proposed implantable antenna at 2.444 GHz, considering various data rates. This analysis is critical in determining the achievable data communication speeds and distances between the transmitter (T_x) and receiver (R_x) antennas. The study indicates that the antenna's performance is adequate for transmitting data at speeds of Br = 7 kbps or 100 kbps. These data rates are considered suitable for the antenna's capabilities based on the analysis provided in reference (Hout & Chung, 2019). The simulated link margin calculation, as illustrated in Figure 10, is a crucial metric for assessing communication quality. The link margin represents the available margin or buffer

between the received signal strength and the minimum required signal strength for reliable communication. Figure 12 shows the link margin calculation results for different data rates, specifically 7 kbps, 100 kbps, and 1 Mbps. The key observation is that a 15 dB link margin is achieved, which signifies that there is a 15 dB surplus of received signal strength over the minimum required for reliable communication. With a 15 dB link margin, the results suggest that 1 Mbps data communication can be reliably established at a distance of approximately 8 meters between the Tx and Rx antennas. This distance represents the effective communication range for the given data rate. Importantly, the communication distance can be extended further when lower data speeds, such as 7 kbps or 100 kbps, are utilized.

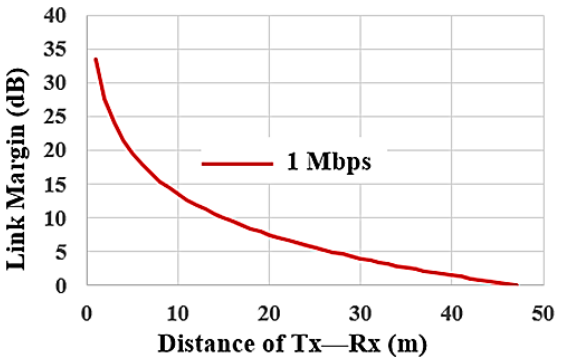

Figure 1: Simulated Link Margin calculation at 2444 MHz in different data rates.

Lower data rates require less signal strength for reliable communication, allowing for increased communication distances. The link margin calculation results highlight the antenna's capability to support reliable data communication at various speeds. With a 15 dB link margin, a 1 Mbps data rate can be sustained at an 8-meter distance between the T_x and R_x antennas. The flexibility to achieve longer communication distances by using lower data rates further enhances the antenna's versatility for various wireless communication applications, taking into account specific data rate requirements and distance constraints.

3.4 Performance Comparision

The Table 5 provides a comprehensive comparison of the proposed implantable antenna's performance with that of several renowned papers from recent literature. This comparative analysis is essential for assessing the antenna's strengths and advantages in terms of size, gain, bandwidth, and specific absorption rate (SAR). The proposed antenna stands out due to its compact size, which is a crucial feature for implantable medical devices (IMD). The antenna's volume is significantly smaller ($5.5 \times 8 \times 1.36$ mm^3) compared to the dimensions of antennas in other references. This compact size is advantageous for implantation within the human body. The proposed antenna exhibits competitive performance in terms of gain and bandwidth. It has a gain of -22.55 dBi, which is within the range of gains reported in the selected references. Additionally, the antenna's bandwidth of 8.72% is

comparable to or better than other designs. A wider bandwidth can accommodate a broader range of frequencies, enhancing the antenna's versatility. Specific absorption rate (SAR) is a critical parameter when assessing the safety of implantable antennas. The SAR values for the proposed antenna are found to be 558 W/kg for the 1-g average and 63.9 W/kg for the 10-g average.

Table 5: Performance Comparison with Some Recent Literatures.

Ref.	Freq. (MHz)	Vol. (mm^3)	Gain (dBi)	BW (%)	SAR (W/Kg)	
					1-g	10-g
Huang & Kishk, (2011)	2400	10 × 10 × 1.5	-20.75	14.9	568.2	84.6
Mitra *et al.*, (2018)	2475	10 × 10 × 1.5	-25	3.23	-	-
Liu *et al.*, (2014)	2400	9.8 × 9.8 × 1.27	-33	21.5	486	90
Singh & Kaur, (2021)	2450	13.3 × 14.6 × 1.92	-17.05	18.10	775.5	-
Darvazehban *et al.*, (2019)	2450	10.2 × 8.61 × 1.92	-17.08	13.7	900	82.1
Proposed	**2444**	**8× 5.5 × 1.36**	**-20.3**	**8.72**	**558**	**61.6**

These SAR values are well within the accepted range and compare favorably with the values reported in references (Singh & Kaur, 2021).Comparing the proposed antenna with the selected references, it's evident that the antenna offers a combination of compact size, competitive gain, and bandwidth, making it suitable for implantable medical devices. Moreover, its SAR values fall within acceptable limits, underscoring its safety for use in biomedical applications. The proposed implantable antenna demonstrates notable advantages in size, performance, and safety when compared to previous designs in the literature. These attributes position it as a promising candidate for use in implantable medical devices where size constraints, gain, bandwidth, and SAR compliance are critical considerations.

4. Conclusion

This study introduces a compact implantable antenna tailored for using within human tissue. The antenna's small dimensions, measuring 8 × 5.5 × 1.36 mm^3, highlight its suitability for implantation in medical devices. Its patch is resemble a dumbbell shape,and its patch and ground is shorted with a shorting pin. The optimized antenna can be resonated at 2.444 GHz band when it is implanted within the three layer(skin, fat, and muscle) of human tissue phantom.The antenna'simpressive performance metrics further solidify its viability. With an almost ideal impedance of 49.87 — j 0.16 Ω, it achieves a favorable voltage standing wave ratio (VSWR) of 1.004. Additionally, the antenna demonstrates noteworthy characteristics, including a broad impedance bandwidth of 213 MHz, a gain of -20.3 dBi, directivity of 6.73 dB, and radiation efficiency of -29.73 dB.The specific absorption rate (SAR) for this antenna is found to be 558 W/kg for 1g of

typical standard tissue and 63.9 W/kg for 10g of average standard tissue.Crucially, the antenna exhibits the ability to establish effective communication with a receiver antenna at distances of approximately 8 meters with 1 Mbps bit rate, underlining its practicality for wireless communication applications within the human body.Overall, this compact implantable antenna combines innovative design features with excellent performance metrics, making it a promising candidate for integration into implantable medical devices.

Acknowledgement

The author expresses gratitude to Founder Prof. Dr. M. Alimullah Miyan and extends special thanks to Professor Mahmuda Khanum and the TN Research Institute in Bangladesh for providing resources from the institute.

References

Darvazehban, A., Rezaeieh, S. A., Zamani, A., & Abbosh, A. M. (2019). Pattern reconfigurable metasurface antenna for electromagnetic torso imaging. *IEEE Transactions on Antennas and Propagation*, *67*(8), 5453-5462.

Duan, Z., Guo, Y. X., Je, M., & Kwong, D. L. (2014). Design and in vitro test of a differentially fed dual-band implantable antenna operating at MICS and ISM bands. *IEEE transactions on antennas and propagation*, *62*(5), 2430-2439.

Gayathri, C., & Venkatanarayanan, S. (2021). A miniaturized circular maze shaped antenna for implantable health care applications. *Journal of Ambient Intelligence and Humanized Computing*, *12*, 4757-4763.

Hendriks, W. A. P. M., Dijkstra, M., Emmerik, C. V., Hegeman, I., & García-Blanco, S. M. (2020, June). High refractive index low-loss aluminium oxide waveguides. In *Eur. Conf. Integr. Opt.(1)* (pp. 2-4).

Hout, S., & Chung, J. Y. (2019). Design and characterization of a miniaturized implantable antenna in a seven-layer brain phantom. *IEEE Access*, *7*, 162062-162069.

Huang, W., & Kishk, A. A. (2011). Embedded spiral microstrip implantable antenna. *International Journal of Antennas and Propagation*, *2011*.

Hussein, S. H., & Mohammed, K. K. (2023). A Review of Miniaturized Advanced IC Rectenna for Energy Harvesting Applications. *Al-Rafidain Engineering Journal (AREJ)*, *28*(1), 145-164.

Kaim, V., Kanaujia, B. K., Kumar, S., Choi, H. C., Kim, K. W., & Rambabu, K. (2020). Ultra-miniature circularly polarized CPW-fed implantable antenna design and its validation for biotelemetry applications. *Scientific reports*, *10*(1), 6795.

Kiourti, A., Costa, J. R., Fernandes, C. A., Santiago, A. G., & Nikita, K. S. (2012). Miniature implantable antennas for biomedical telemetry: From simulation to realization. *IEEE Transactions on Biomedical Engineering*, *59*(11), 3140-3147.

Kiourti, A., & Nikita, K. S. (2012). A review of implantable patch antennas for biomedical telemetry: Challenges and solutions [wireless corner]. *IEEE Antennas and Propagation Magazine*, *54*(3), 210-228.

Lee, J. H., Seo, D. W., & Lee, H. S. (2015, November). Design of implantable antenna on the dielectric/ferrite substrate for wireless biotelemetry. In *2015 International Symposium on Antennas and Propagation (ISAP)* (pp. 1-3). IEEE.

Liu, C., Guo, Y. X., & Xiao, S. (2014). Capacitively loaded circularly polarized implantable patch antenna for ISM band biomedical applications. *IEEE transactions on antennas and propagation*, *62*(5), 2407-2417.

Loktongbam, P., Pal, D., & Koley, C. (2020). Design of an implantable antenna for biotelemetry applications. *Microsystem Technologies*, *26*(7), 2217-2226.

Mainul, E. A., & Hossain, M. F. (2021). A Miniaturized Triple Band DGS Implantable Antenna for Biotelemetry. In *2021 International Conference on Electrical, Communication, and Computer Engineering (ICECCE)* (pp. 1-6). IEEE.

Mainul, E. A., & Hossain, M. F. (2021). Design of a Compact Implantable Antenna in Seven-layer Brain Phantom for Brain-machine Interface Applications. In *2021 International Conference on Electronics, Communications and Information Technology (ICECIT)* (pp. 1-4). IEEE.

Mitra, D., Das, S., & Paul, S. (2019, March). SAR reduction for an implantable antenna using ferrite superstrate. In *2019 International Workshop on Antenna Technology (iWAT)* (pp. 1-4). IEEE.

Moore, R. (1963). Effects of a surrounding conducting medium on antenna analysis. *IEEE Transactions on Antennas and Propagation*, *11*(3), 216-225.

Shah, S. A. A., & Yoo, H. (2018). Scalp-implantable antenna systems for intracranial pressure monitoring. *IEEE Transactions on Antennas and Propagation*, *66*(4), 2170-2173.

Singh, G., & Kaur, J. (2021). Skin and brain implantable inset-fed antenna at ISM band for wireless biotelemetry applications. *Microwave and Optical Technology Letters*, *63*(2), 510-515.

Soliman, M. M., Chowdhury, M. E., Khandakar, A., Islam, M. T., Qiblawey, Y., Musharavati, F., & Zal Nezhad, E. (2021). Review on medical implantable antenna technology and imminent research challenges. *Sensors*, *21*(9), 3163.

Stutzman, W. L., & Thiele, G. A. (2012). *Antenna theory and design*. John Wiley & Sons.

Sukhija, S., & Sarin, R. K. (2017). Low-profile patch antennas for biomedical and wireless applications. *Journal of Computational Electronics*, *16*, 354-368.

Valanarasi, A., & Dhanasekaran, R. (2020). Optimum band ε shaped miniature implantable antennas for telemetry applications. *IEEE Transactions on Antennas and Propagation*, *69*(1), 55-63.

Van Lith, M., Zakavi, P., Karmakar, N. C., & Griggs, I. (2009). Wireless orthopaedic pin for bone healing and growth: antenna developement. In *Annual Conference on Engineering and Physical Sciences in Medicine/Australian Biomedical Engineering Conference 2009*.

Xu, L. J., Jin, X., Hua, D., Lu, W. J., & Duan, Z. (2020). Realization of circular polarization and gain enhancement for implantable antenna. *IEEE Access*, *8*, 16857-16864.